Int. J. Solids Structures, 1971, Vol. 7, pp. 559 to 584. Pergamon Press. Printed in Great Britain

STRESS ANALYSIS OF HEXAGONAL SHELLS†

DUSAN KRAJCINOVIC

Argonne National Laboratory, Argonne, Illinois

Abstract—A convenient method for the stress analysis of long prismatic shells with hexagonal cross sections, subjected to static loading, is developed. By employing the semi-membrane method in conjunction with a variational principle a closed form solution is obtained. It is, therefore, easy to perform a parametric study of the influence of various geometries and boundary conditions on the state of stress. Among other things, it is shown that stiffening the shell with cross-sectional diaphragms is not always advisable.

NOTATION

A	cross-sectional area
$a_{ij}, b_{ij}, c_{jk}, r_{hk}, s_{hk}$	certain definite integrals defined by (2.4)
D	flexural rigidity of the plate
d	thickness of a plate
E	elastic modulus
$F(\xi)$	functions defined by (4.2)
$[F]$	field transfer matrix
G	shear modulus
I_y	principal moment of inertia of the hexagonal cross section (in.^{4})
I_ω	sectorial moment of inertial (in.^{6})
K	a cross sectional parameter (in.^{4})
K_κ	flattening moment of inertia (in.^{2})
L	length of the shell
l	width of a plate in the cross section
M_s, M_z, M_{zs}	bending moments and torsional moment in a plate (lb in.)
M_y	bending moment of a shell regarded as a beam (lb in.)
M_ω	bimoment (lb in.^{2})
m_ω	nondimensional bimoment (3.21)
N_z, N_s, N_{zs}	normal and shear forces (lb)
p_z, p_s, p_n	external loads in direction of coordinate axes (lb in.$^{-2}$)
p_κ	flattening load (lb)
Q_κ	flattening force (lb in.)
q_κ	nondimensional flattening force (3.21)
$r, \bar{s}$	nondimensional parameters defined by (3.9)
$\{S\}$	state vector
s	circumferential coordinate
T	temperature rise above the reference state
$u(z, s)$	displacement in the longitudinal direction (in.)
$U_i(z)$	generalized coordinate
$v(z, s)$	displacement in the circumferential direction (in.)
$V_i(z)$	generalized coordinate
x, y, z	coordinate frame
W	total potential energy
α, β	nondimensional parameters (4.3)
α_t	thermal coefficient of linear expansion
ε	dilatation

† Work performed under the auspices of the U.S. Atomic Energy Commission.

κ_1, κ	flattening (nondimensional)
ν	Poisson's ratio
$\xi = z/L$	nondimensional longitudinal coordinate
σ_z, σ_s	normal stress (lb in.$^{-2}$)
$\rho = L/l$	relative length ratio
τ	shearing stress (lb in.$^{-2}$)
ϕ, ψ	deformation modes
$\Psi = \psi_2$	cross sectorial coordinate (in.)
$\Omega = \phi_3$	sectorial coordinate (in.^{2})
ω_1	warping (in.$^{-1}$)
ω	nondimensional warping (3.21)

INTRODUCTION AND BACKGROUND

CURRENT core design concepts for Sodium Cooled Fast Breeder Reactors emphasize honeycomb arrays of subassembly ducts, each containing hundreds of fuel pins. The subassembly duct is commonly of thin walled hexagonal cross section and is long with respect to the distance across flats. The space between fuel pins inside the duct and the required clearance space between ducts is filled with liquid sodium.

Within the wide range of problems being studied for the purpose of assessing reactor safety is an important set of structural response problems associated with known and postulated accident mechanisms initiated within a subassembly duct. Such accidents include local and total flow blockage within a subassembly, voiding due to vapor generation and coolant expulsion and reentry pressures initiated by blockage and/or fuel pin clad failures leading to the injection of molten fuel into the coolant. Within this context the structural response study is intended to develop methods for estimating the confinement potential of a single duct to such postulated accidents and then to examine the response of surrounding ducts should this confinement potential be exceeded. This paper is concerned with one part of the total long range study, namely the static stress analysis of a typical subassembly duct subjected to lateral pressure (Fig. 1) in order to understand the coupling between gross lateral bending and cross sectional deformation.

1. FORMULATION OF THE PROBLEM

We consider a long prismatic shell with a hexagonal cross section (Fig. 1). Six identical plates are rigidly joined together along the nodal lines. The shell is subjected to a lateral load $p_n(z)$ which is for convenience considered to be symmetric with respect to y axis. The shell is surrounded by a stationary temperature field giving rise to moderate thermal stresses. The boundary conditions on two terminal cross sections are considered to be natural but are otherwise arbitrary.

The proposed goal is to establish a rather simple but sufficiently accurate method of analysis for the considered shell. The method is expected to allow for a qualitative analysis in order to estimate the influence of shell's geometry and boundary conditions on the state of stress. In addition, an extension of the analysis to stability and vibration problems should be attainable.

In addition to some purely numerical solutions the considered shell may be analyzed as a folded structure (using either mixed or displacement method—see Ref. [1]) or as a

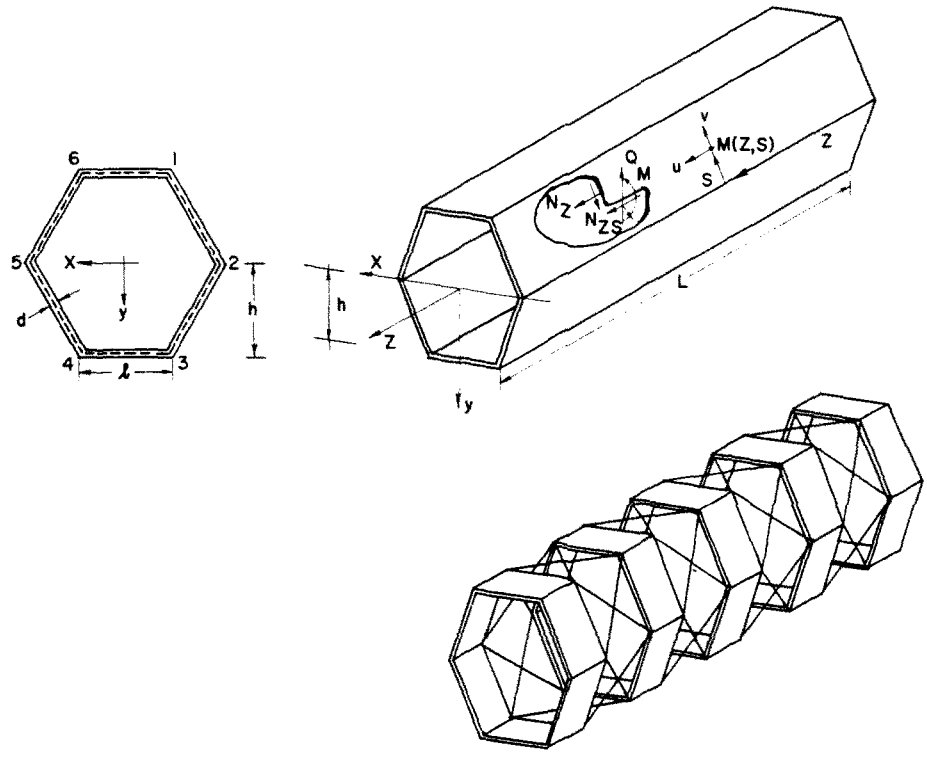

FIG. 1. Subassembly fuel duct (a) cross section, (b) non-zero forces and displacements, (c) analytical model.

thinwalled structure employing the so called semimembrane theory (or Vlasov's variational approach).

The essence of the latter method (see Refs. [2, 3]) is that the variations of all displacements and stresses in the direction of the generatrix are assumed to be smoother than those in circumferential direction. In other words, the bending moment M_z, torsional moment M_{zs} and the transverse force Q_z are neglected. These forces are considered to be of secondary importance in comparison with the rest of the internal forces presented in Fig. 1. As far as the kinematics of the deformation is concerned we assume that each plate for itself deforms according to Bernoulli's hypothesis. The physical meaning of introduced assumptions is that the actual shell is approximated by a spatial system consisting of hexagonal frames joined together by a lattice structure [Fig. 1(c)].

The position of an arbitrary point M on the middle surface is determined by coordinate z from a fixed cross section and by the circumferential coordinate s (measured counter-clockwise from an *a priori* determined generatrix $s = 0$). The deformed position of the shell's middle surface is determined if the displacement of each point is a known function of z and s.

We denote by $u(z, s)$ the component of the displacement vector along the longitudinal axis and by v the component in the circumferential axis. Positive directions of u and v are indicated on Fig. 1.

The basic feature of the employed Vlasov's method is that the displacement components u and v are approximated by finite series

$$u(z, s) = \sum_{i=1}^{n} U_i(z)\phi_i(s)$$
$$v(z, s) = \sum_{k=1}^{n} V_k(z)\psi_k(s) \tag{1.1}$$

where $U_i(z)$ and $V_k(z)$ are generalized coordinates to be solved for, while $\phi(s)$ and $\psi(s)$ are some *a priori* chosen (known) deformation modes. Such a technique apparently serves to reduce the governing system of partial differential equations to a corresponding system of ordinary differential equations.

As a consequence of our assumptions concerning the deformation of the cross section the axial displacements are fully determined by six axial nodal displacements. If we restrict ourselves to deformations symmetric with respect to y coordinate, the total number of unknown generalized coordinates U_i is apparently $m = 3$.

The number of unknown functions V_k depends on our choice. There are, obviously, three rigid body degrees of freedom for an arbitrary cross section (two displacement components and a rotation about the longitudinal axis). In addition, one may wish to consider distortions of cross section likely to occur for the specific load. We again restrict ourselves to deformations symmetric with respect to y-axis, which reduces the number of rigid body motions to one (vertical displacement), and assume that the shell may experience flattening. The reason for such an assumption, in case of the considered load, is apparent after the load is presented as a superposition of its symmetric and antisymmetric part. The latter one is obviously associated with pure distortion without bending in longitudinal direction since its resultant vanishes.

It is obvious that the choice of five deformation modes ϕ_i and ψ_i is rather arbitrary (as long as they are independent). It is convenient to choose them as shown in Fig. 2. Mode ϕ_1 corresponds to the axial displacement, mode ϕ_2 to conventional beam flexure (rotation about x-axis), mode ϕ_3 to deplanation (similar to what is in torsion problems called warping† although definitively not the same), mode ψ_1 to vertical displacement and mode ψ_2 to the flattening. Modes ϕ_1, ϕ_2 and ψ_1 define the deformation of the shell treated as a beam in conventional sense (Bernoulli's hypothesis valid), while ϕ_3 and ψ_2 reflect deformations associated with the longitudinal and transverse distortion of the cross section. In other words modes ϕ_3 and ψ_2 result from the fact that the shell's cross section is regarded to be too flexible to deform according to Bernoulli's hypothesis.

The diagrams of the deformation modes ϕ_i and ψ_i are plotted in Figs. 3 and 4. Plotted are also first derivatives $\mathrm{d}\phi_i/\mathrm{d}s$. For the assumed positive directions of the coordinates s it follows that

$$\frac{\mathrm{d}\phi_i}{\mathrm{d}s} = \frac{\partial\phi_i}{\partial x}\frac{\mathrm{d}x}{\mathrm{d}s} + \frac{\partial\phi_i}{\partial y}\frac{\mathrm{d}y}{\mathrm{d}s} = -\frac{\partial\phi_i}{\partial x}\sin\alpha + \frac{\partial\phi_i}{\partial y}\cos\alpha.$$

Since

$$\phi_1 = 1 \qquad \phi_2 = y \qquad \phi_3 = -\tfrac{2}{3}h^2 + hy\,.\,\mathrm{sgn}(y) \tag{1.2}$$

† We will henceforth use the term "warping" although in classical sense of warping torsion the considered shell does not warp (due to the fact that $\mathrm{d}h = \mathrm{const.}$).

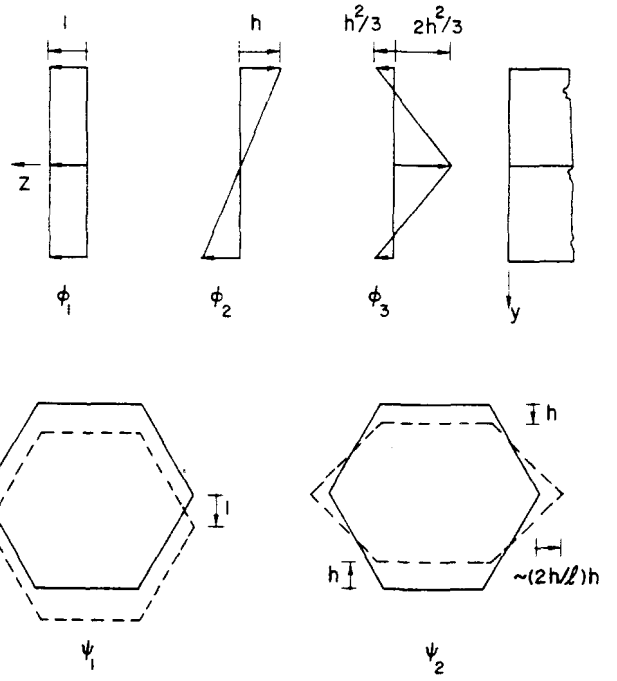

FIG. 2. Assumed longitudinal and transverse deformation modes.

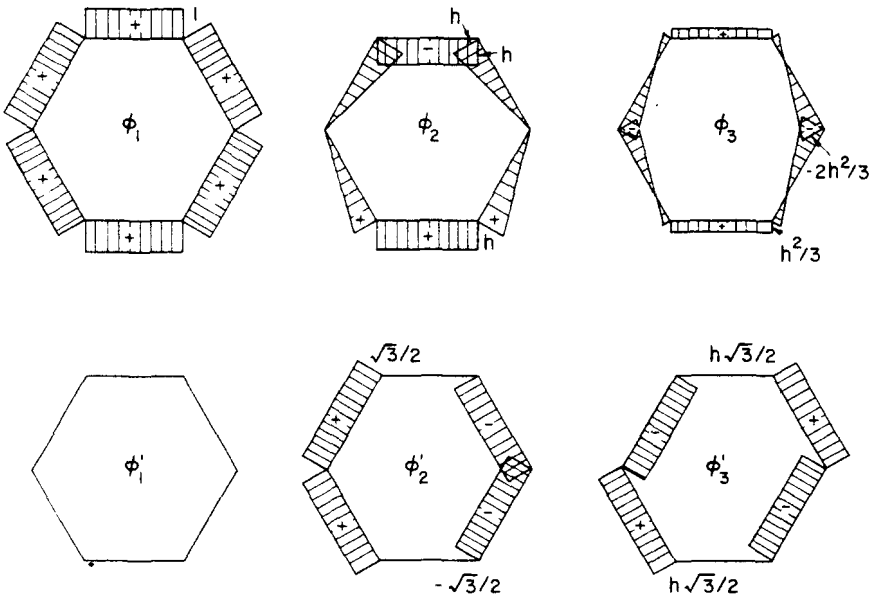

FIG. 3. Diagrams of longitudinal deformation modes and its derivatives with respect to s.

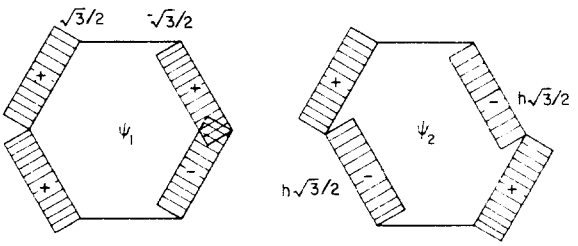

FIG. 4. Diagrams of transverse deformation modes.

one has

$$\frac{d\phi_1}{ds} = 0 \qquad \frac{d\phi_2}{ds} = \cos\alpha \qquad \frac{d\phi_3}{ds} = h \,.\, \cos\alpha\, \mathrm{sgn}(y)$$

Note also that since the functions ψ_i are constant along each plate length, $d\psi_i/ds \equiv 0$.

2. DIFFERENTIAL EQUATIONS—GENERAL DERIVATION

The external load acting upon the shell is presented by its three components p_z, p_s and p_n in direction of three coordinate axes z, s and normal to the middle surface n. In order to be consistent with the proposed model the external load is decomposed into two components: (a) a self-equilibrated system of forces bending the hexagonal frame without displacing its mass center, and (b) a system of concentrated nodal loads causing the vertical displacement of the frame (and, therefore, stressing the lattice structure).

For example, consider uniformly distributed load given in Fig. 5(a). Decompose it into a system of resultant nodal forces [Fig. 5(c)] and a self-equilibrated load [Fig. 5(b)]. From the standpoint of our frame–lattice model it is apparent that the latter component having no resultant only bends (distorts) the cross-sectional frame. The system of nodal forces [Fig. 5(c)] has a two-fold action: firstly it bends the shell as a beam (without distorting its cross sections—only normal forces in the lattice do exist) and it secondly adds to the distortion of the cross section through its components p_{si} in the direction of individual plates [Fig. 5(d)].

The stresses in the shell are

$$\begin{aligned} \sigma_z &= E\varepsilon_z = E\frac{\partial u}{\partial z} = E\sum_i U_{i,z}\phi_i \\ \tau_{sz} &= G\left(\frac{\partial u}{\partial s} + \frac{\partial v}{\partial z}\right) = G\left(\sum_i U_i\phi_{i,s} + \sum_k V_{k,z}\psi_k\right) \end{aligned} \tag{2.1}$$

where the following symbolism is introduced

$$U_{i,z} = \frac{\partial U_i}{\partial z}$$

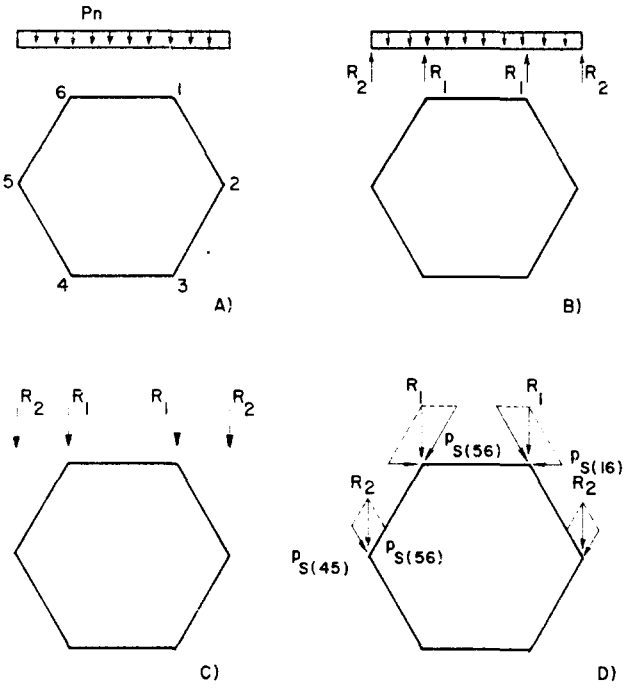

FIG. 5. Decomposition of the lateral load p_n into a self-equilibrated load and a load with resultant.

The forces in the shell are accordingly

$$N_z = \frac{Ed}{1-\nu^2}\left[\frac{\partial u}{\partial z}+\nu\frac{\partial v}{\partial s}-(1+\nu)\alpha_t T\right]; N_{zs} = \frac{Ed}{2(1+\nu)}\left(\frac{\partial u}{\partial s}+\frac{\partial v}{\partial z}\right)$$
$$N_s = \frac{Ed}{1-\nu^2}\left[\frac{\partial v}{\partial s}+\nu\frac{\partial u}{\partial z}-(1+\nu)\alpha_t T\right]; M_s = -D\frac{\partial^2 w}{\partial s^2} \tag{2.2}$$

where E is the elastic modulus, G shear modulus, ν Poisson's ratio, α_t thermal coefficient of linear expansion, T the temperature rise above the reference state, d thickness of each individual plate, $D = Ed^3/12(1-\nu^2)$ the flexural rigidity of the plate and w the displacement along the normal to the middle surface of the shell.

The total potential energy is the sum of the strain energy of the lattice, strain energy of the frame (in bending) and the potential energy of external load

$$W = \int_0^L \left\{ \int_s [\tfrac{1}{2}(N_z\varepsilon_z + N_s\varepsilon_s + N_{zs}\gamma_{zs} + M_s\kappa_s) - (p_z u + p_s v)]\,\mathrm{d}s - \sum p_{si}v_i \right\} \mathrm{d}z \tag{2.3}$$

where M_s is the bending moment and $\kappa_s = M_s/D$ the rotation of the cross section of the frame, p_{si} forces given in Fig. 5(d) and v_i tangential displacement of the plate i.

After substitution of (2.1) and (2.2) into (2.3) obtained are the governing Euler's equations

of the problem rendering the potential energy minimum.

$$\sum_i \left(U_{i,zz} a_{ij} - \frac{1-\nu}{2} U_i b_{ij} \right) - \frac{1-\nu}{2} \sum_k V_{k,z} c_{jk} - (1+\nu)\alpha \sum_i t_{i,z} a_{ij} + \frac{1-\nu^2}{E} p_{jz} = 0$$
$$\frac{1-\nu}{2} \sum_i U_{i,z} c_{ih} + \frac{1-\nu}{2} \sum_k (V_{k,zz} r_{kh} - V_k s_{kh}) - \frac{1-\nu^2}{E} p_{hs} = 0 \tag{2.4}$$

with comma standing for differentiation with respect to the argument following it. Introduced is also the notation

$$a_{ij} = \int \phi_j \phi_i \, dA \qquad r_{hk} = \int \psi_h \psi_k \, dA$$
$$b_{ij} = \int \phi_{j,z} \phi_{i,z} \, dA \qquad s_{hk} = \frac{1}{E} \int \frac{M_h(s) M_k(s)}{EI} \, ds \tag{2.5}$$
$$c_{jk} = \int \phi_{j,z} \psi_k \, dA$$

and

$$p_{jz} = \int p_z \phi_j \, ds \qquad p_{hs} = \int p_s \psi_h \, ds + \sum_{(ij)} p_{s(ij)} \psi_{h(ij)}. \tag{2.6}$$

Coefficients t_i are calculated in the following way. We first present the temperature distribution in form of series

$$T = \sum_i t_i(z) \phi_i(s) \tag{2.6}$$

and then determine $t_i(z)$ simply as solutions of the set of linear algebraic equations

$$\sum_i t_i a_{ij} = \int_s T \phi_j \, dA.$$

Since a_{ij} are in most cases orthogonal the solution for t_i is straightforward.

The associated boundary conditions are derived to be

$$\int_s N_z \phi_j \, ds - \int_s N_z^* \phi_j \, ds = 0$$
$$\int_s N_{sz} \psi_h \, ds - \int_s N_{sz}^* \psi_h \, ds = 0 \tag{2.7}$$

where asterisk indicates external force applied to the structure. Integration is carried out over the entire terminal cross section.

3. DIFFERENTIAL EQUATION FOR THE HEXAGONAL SHELL—SYMMETRIC CASE

As a first step of specifying equations (2.4) for the symmetric deformation of a hexagonal shell we compute the integrals (2.5) and (2.6) using the diagrams for modes ϕ_1 and ψ_h as given in Figs. 3 and 4.

We write only nonzero terms

$$\begin{aligned} a_{11} &= \int 1^2\,\mathrm{d}A = 6d = A & c_{21} &= 3\,\mathrm{d}l = \tfrac{1}{2}A \\ a_{22} &= \int y^2\,\mathrm{d}A = I_y & c_{32} &= -3\,\mathrm{d}h^2 l = -K \\ a_{33} &= \tfrac{2}{3}\,\mathrm{d}h^4 l = I_\omega & r_{11} &= 3\,\mathrm{d}l = \tfrac{1}{2}A \\ b_{22} &= 3\,\mathrm{d}l = \tfrac{1}{2}A & r_{22} &= 3\,\mathrm{d}h^2 l = K \\ b_{33} &= 3\,\mathrm{d}h^2 l = K \end{aligned} \tag{3.1}$$

where A is the cross-sectional area, I_y moment of inertia about x-axis, I_ω sectorial moment of inertia (with the dimension of in.^{6}), such that EI_ω is the warping rigidity (resistance to warping) while GK is the shear rigidity.

Finally we compute the term $\sum_i V_k \int (M_k M_h/EI)\,\mathrm{d}s$ expressing the work of internal forces associated with the flattening of the cross sectional frame. The diagram of bending moments due to $V_2(z) = 1$ (Fig. 2) is plotted in Fig. 6(a). The moment in the node is computed to be

$$M_s = \frac{24}{5}\frac{EI}{l}\frac{h}{l} \tag{3.2}$$

therefore

$$s_{22} = \frac{1}{E}\int \frac{M^2}{EI}\,\mathrm{d}s = \frac{384}{5}\frac{I}{l}\left(\frac{h}{l}\right)^2 = \frac{32}{5}\frac{d^3}{l}\left(\frac{h}{l}\right)^2 = K_\kappa$$

since the moment of inertia for the frame is

$$I = \tfrac{1}{12}d^3.$$

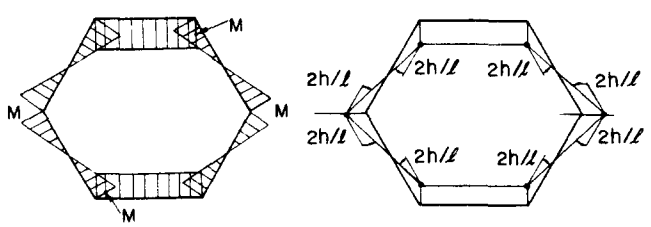

FIG. 6. Moment diagram in the hexagonal frame corresponding to the flattening of the cross section.

Coefficient s_{22} has been determined as a generalized reaction of the cross-sectional frame to deformation $V_2 = 1$, and, therefore, represents the rigidity of the frame against flattening. Thus cross-sectional parameter K_κ will be referred to as flattening moment of inertia (in.^{2}).

For the uniform lateral load p_n (as shown in Fig. 5) concentrated nodal forces R are

$$R_1 = \frac{3p_n l}{4} \quad \text{and} \quad R_2 = \frac{p_n l}{4}.$$

Hence,

$$p_s(56) = \frac{1}{\sqrt{3}} p_n l \qquad p_{s(45)} = \frac{1}{4\sqrt{3}} p_n l$$

The distributed load in the plane of the plate

$$p_s = \frac{1}{l} p_{2t} = \frac{\sqrt{3}}{4} p_n$$

According to (2.6)

$$p_{s1} = \int p_s \psi_1 \, ds + \sum p_{s(ij)} \psi_{1(ij)} = 2p_n l$$

$$p_{s2} = \int p_s \psi_2 \, ds + \sum p_{s(ij)} \psi_{2(ij)} = \tfrac{3}{2} p_n l h. \tag{3.3}$$

The first of two forces, corresponding to vertical displacement, equals exactly the distributed transverse load, as one certainly may have expected. The second force p_{s2} may be referred to as a distributed flattening force.

Once all the necessary coefficients are computed, the governing system of equations is written from (2.4) as

$$\begin{aligned}
EAU_1'' - E\alpha t_1' A + p_{z1} &= 0 \\
EI_y U_2'' - \tfrac{1}{2} GAU_2 - \tfrac{1}{2} GAV_1' - \alpha EI_y t_2' + p_{z2} &= 0 \\
EI_\omega U_3'' - GKU_3 + GKV_2' - \alpha EI_\omega t_3' + p_{z3} &= 0 \\
\tfrac{1}{2} GAU_2' + \tfrac{1}{2} GAV_1'' + p_{s1} &= 0 \\
-GKU_3' + GKV_2'' - EK_\kappa V_2 + p_{s2} &= 0
\end{aligned} \tag{3.4}$$

where for convenience $\nu = 0$. With primes denoted are the derivatives with respect to z.

It is apparent that for the assumed deformation modes the state of stress may be regarded as a superposition of three independent states:

(a) Axial loading

$$EAU_1'' = -p_{z1} - EA\alpha t_1' \tag{3.5}$$

(b) Bending in the principal plane yz

$$\begin{aligned}
EI_y U_2'' - \tfrac{1}{2} GA(U_2 + V_1') + p_{z2} - \alpha EI_y t_2' &= 0 \\
\tfrac{1}{2} GA(U_2' + V_1'') + p_{s1} &= 0
\end{aligned}$$

or simply with $V_1 = \eta(z)$.

$$EI_y\eta^{1V} = p_{s1} - 2\frac{EI_y}{AG}p''_{s1} - p'_{z2} + \alpha EI_y(t'_2)'. \tag{3.6}$$

The second and third term on the right-hand side of equation (3.6) reflects the influence of shearing stresses in the plane of plates on the deformation of the member. If they are neglected equation (3.6) is identical to the well known equation of beam flexure.

(c) Distortion of the cross section

$$\begin{aligned} EI_\omega\omega''_1 - GK(\omega_1 - \kappa'_1) + p_\omega &= 0 \\ -GK(\omega'_1 - \kappa''_1) - EK_\kappa\kappa_1 + p_\kappa &= 0 \end{aligned} \tag{3.7}$$

where the symbol $\omega_1(\text{in.}^{-1})$ is used for the "warping" U_3 of the cross section, while for the flattening V_2 a new symbol κ_1 (nondimensional) is used. Also

$$p_\omega = p_{z3} \text{ and } p_\kappa = p_{s2}.$$

Using nondimensional quantities $\omega = \omega_1 l$ and $\xi = z/L$, with L being, say, span of the shell, from (3.7) it follows

$$\omega^{1V} - 2r^2\omega'' + s^4\omega = p \tag{3.8}$$

where the differentiation is now with respect to ξ. Nondimensional parameters r and s are given by

$$r^2 = \frac{1}{2}\frac{EK_k}{GK}L^2 = \frac{32}{15}\left(\frac{d}{l}\right)^2\left(\frac{L}{l}\right)^2 \quad \text{and} \quad s^4 = \frac{K_k}{I_\omega}L^4 = \frac{64}{5}\left(\frac{d}{l}\right)^2\left(\frac{L}{l}\right)^4 \tag{3.9}$$

while the right hand side p is

$$p = \frac{K_\kappa}{I_\omega}L^4 l p_\omega - \frac{L^4 l}{EI_\omega}p''_\omega + \frac{L^4 l}{EI_\omega}p'_\kappa. \tag{3.10}$$

The flattening of the cross section κ_1, written in terms of ω_1 is

$$\kappa_1 = -\frac{I_\omega}{K_\kappa}\frac{\mathrm{d}^3\omega_1}{\mathrm{d}z^3} + \frac{1}{EK_\kappa}(p_\kappa - p'_\omega). \tag{3.11}$$

Introduce generalized force

$$P_j = -\int_A \sigma\phi_j(s)\,\mathrm{d}A \tag{3.12}$$

From $\sigma_z = E\varepsilon_z = Eu_{,z}$ we write

$$P_j = -E\sum_i U_{i,z}\int^z \phi_j\phi_i\,\mathrm{d}A$$

If, finally, functions ψ_i are chosen to be orthogonal (as in our case they actually are), the generalized forces are

$$p_j = EU_{j,z}a_{jj} \tag{3.13}$$

i.e. the normal stress σ_z is given by

$$\sigma_z(z, s) = \sum_i \frac{P_i(z)}{a_{ii}} \phi_i(s). \tag{3.14}$$

From (3.12) we calculate

$$P_1 = -\int \sigma_z \, dA = N_z \qquad P_2 = -\int \sigma_z y \, dA = M_y$$

and

$$P_3 = M_\omega = -\int \sigma_z \phi_3 \, dA = -EI_\omega \omega' \tag{3.15}$$

where $I_\omega = a_{33}$ is given by (3.1).

Hence

$$\sigma = \frac{N}{A} + \frac{M_y}{I_y} y + \frac{M_\omega}{I_\omega} \Omega \tag{3.16}$$

where the first two terms represent the normal stress calculated from the beam theory (3.5) and (3.6), while the last term is the contribution of the cross-sectional distortion. Due to the similarity with the thin-walled member torsion problems (see Refs. [4, 5]) we will refer to M_ω (lb in.^{2}) as bimoment (see Fig. 7), $\Omega = \phi_3$ (in.^{2}) as sectorial coordinate and $I_\omega = \int \Omega^2 \, dA$ (in.^{6}) as sectorial moment of inertia.

The generalized force associated with flattening is

$$Q_\kappa = \int_A \tau \psi_2 \, dA = G(U_3 \int \phi_3' \psi_2 \, dA + V_2' \int \psi_2^2 \, dA)$$

or, using already computed integrals (3.1),

$$Q_\kappa = GK(\kappa_1' - \omega_1). \tag{3.17}$$

The contribution of the flattening due to the shear stress is,

$$\tau_\kappa = G(\kappa_1' - \omega_1)\Psi = \frac{Q_\kappa}{K} \Psi \tag{3.18}$$

where $\phi_3' = -\psi_2 = -\Psi$ is the cross sectorial coordinate. Q_κ (lb in.) will be referred to as the flattening force (Fig. 7).

We also note from (3.7a) that in absence of the distributed external force p_ω,

$$M_\omega' = Q_\kappa \tag{3.19}$$

In other words the relation between the bimoment M_ω and the flattening force Q_κ is identical to the relation between the bending moment and transverse force in conventional beam analysis.

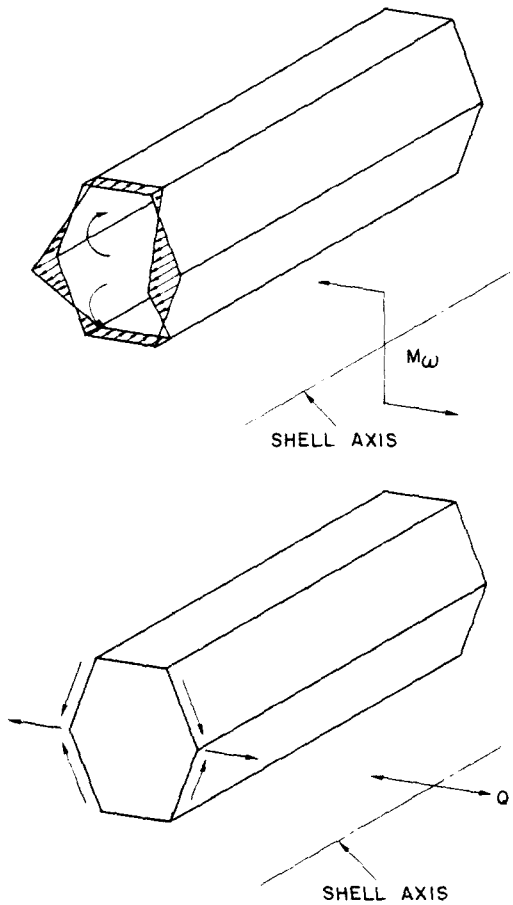

FIG. 7. Bimoment M_ω and flattening force Q_κ.

We finally derive the expressions for M_ω and Q_κ given in terms of ω_1 only

$$M_\omega = -EI_\omega \frac{d\omega_1}{dz}$$
$$Q_\kappa = -EI_\omega \frac{d^2\omega_1}{dz^2} - p_\omega. \tag{3.20}$$

Introducing nondimensional quantities

$$m_\omega = M_\omega \frac{Ll}{EI_\omega}$$
$$q_\kappa = Q_\kappa \frac{L^2 l}{EI_\omega} \tag{3.21}$$
$$\kappa = \kappa_1 \frac{K_\kappa}{I_\omega} lL^3$$

and

$$\bar{p}_\omega = p_\omega \frac{lL^2}{EI_\omega}; \qquad \bar{p}_\kappa = p_\kappa \frac{lL^3}{EI_\omega}. \tag{3.22}$$

We finally write

$$\begin{aligned} m_\omega &= -\omega' \\ q_\kappa &= -\omega'' - \bar{p}_\omega \\ \kappa &= \omega''' + \bar{p}_\kappa - \bar{p}_\omega'. \end{aligned} \tag{3.23}$$

The problem of stress analysis is therefore reduced to the solution of an ordinary differential equation (3.8) with constant coefficients. The resulting stresses are to be superimposed on the stresses due to the flexure and axial stressing (in conventional sense) for which the shell is regarded to be a beam deforming according to Bernoulli's hypothesis.

It is probably appropriate to discuss briefly the choice of the deformation modes ϕ_i and ψ_k. It is realized that only ϕ_1, ϕ_2 and ψ_1 are associated with stress resultants which are to equilibrate the external loads. All subsequent deformation modes should be chosen such as to result in self-equilibrated forces. Instead of assuming, for instance, that the displacement $u(z, s)$ is defined as a straight line between two nodal points, we may feel that the distribution is better approximated by a parabolic (or sinusoidal) curve for which the total area under the curve is vanishing (in order to have orthogonal functions ϕ_i). It is understood, of course, that each additional mode results in an additional equation (and additional unknown generalized displacement and generalized force). In other words additional refinements are paid for by additional computational complexities. The point is, however, that such a trade-off is available if considered justified.

4. SOLUTION

4.1 *General solution of the homogeneous equation*

The solution of the equation (3.8) can be written as

$$\omega(\xi) = c_1 F_1(\xi) + c_2 F_2(\xi) + c_3 F_3(\xi) + c_4 F_4(\xi) \tag{4.1}$$

where c_i are some constants to be determined from boundary conditions, while $F_i(\xi)$ are

$$\begin{aligned} F_1(\xi) &= \cosh \alpha\xi \sin \beta\xi \\ F_2(\xi) &= \cosh \alpha\xi \cos \beta\xi \\ F_3(\xi) &= \sinh \alpha\xi \cos \beta\xi \\ F_4(\xi) &= \sinh \alpha\xi \sin \beta\xi \end{aligned} \tag{4.2}$$

where

$$\alpha = \left(\frac{s^2 + r^2}{2}\right)^{1/2} \qquad \beta = \left(\frac{s^2 - r^2}{2}\right)^{1/2}. \tag{4.3}$$

A particularly convenient way to solve the problem for a variety of boundary conditions is the so called method of initial parameters (see for example Ref. [6]). Coefficients c_i are determined such that the solution (4.1) takes the following form

$$\omega(\xi) = \omega_0 f_1 + \kappa_0 f_2 + m_0 f_3 + q_0 f_4 \tag{4.4}$$

where subscript "0" indicates the value of the corresponding function at the origin $\xi = 0$. Functions f_1 form an independent linear set of functions of particular integrals $F_i(\xi)$. After some elementary calculations it follows from (4.1) and (3.23), that

$$\begin{aligned} \omega_0 &= c_2 & q_0 &= -c_2(\alpha^2-\beta^2)-c_4 2\alpha\beta \\ m_0 &= c_1\beta - c_3\alpha & \kappa_0 &= c_1\beta(3\alpha^2-\beta^2)+c_3\alpha(\alpha^2-3\beta^2) \end{aligned}$$

and, thus

$$\begin{aligned} c_1 &= \alpha\Delta[-\kappa_0-(\alpha^2-3\beta^2)m_0] & c_3 &= \beta\Delta[\kappa_0+(3\alpha^2-\beta^2)m_0] \\ c_2 &= \omega_0 & c_4 &= \frac{1}{2\alpha\beta}[q_0+(\alpha^2-\beta^2)\omega_0] \end{aligned} \tag{4.5}$$

where

$$\Delta = -[2\alpha\beta(\alpha^2+\beta^2)]^{-1}. \tag{4.6}$$

Substituting relations (4.5) back into (4.1) and appropriate relations for m_ω, q_κ and κ, it follows that the so called state vector $\{s\}$,

$$\{s\}_z = [\omega, \kappa, m_\omega, q]^t \tag{4.7}$$

(where superscript t stands for transposition), at an arbitrary position ξ, may be written in terms of the initial state vector (at $\xi = 0$), by means of the field transfer matrix $[F]$, as

$$\{s\} = [F]\{s_0\}. \tag{4.8}$$

The terminology is apparently borrowed from the Ref. [6].

The field transfer matrix $[F]$ is after some simple calculations determined to be

$$[F] = \begin{bmatrix} F_2-\gamma F_4 & -\Delta(\alpha F_1-\beta F_3) & \Delta(b_3F_3-a_3F_1) & -\frac{1}{2\alpha\beta}F_4 \\ -\frac{(\alpha^2+\beta^2)^2}{2\alpha\beta}\times(\alpha F_1+\beta F_3) & F_2+\gamma F_4 & \frac{(\alpha^2+\beta^2)^2}{2\alpha\beta}F_4 & \frac{-1}{2\alpha\beta}(a_3F_1+b_3F_3) \\ \frac{\alpha^2+\beta^2}{2\alpha\beta}\times(\alpha F_1-\beta F_3) & -\frac{1}{2\alpha\beta}F_4 & F_2-\gamma F_4 & \frac{1}{2\alpha\beta}(\alpha F_1+\beta F_3) \\ \frac{(\alpha^2+\beta^2)^2}{2\alpha\beta}F_4 & -\frac{1}{2\alpha\beta}(\alpha F_1+\beta F_3) & -\frac{\alpha^2+\beta^2}{2\alpha\beta}(\alpha F_1-\beta F_3) & F_2+\gamma F_4 \end{bmatrix} \tag{4.9}$$

where

$$\gamma = \frac{\alpha^2 - \beta^2}{2\alpha\beta}$$

$$a_3 = \alpha(\alpha^2 - 3\beta^2) \tag{4.10}$$

$$b_3 = (3\alpha^2 - \beta^2)\beta.$$

4.2 *Particular solution*

Although the discontinuities in distortion ω and κ could also be treated within the presented scheme as some generalized loads we will confine ourselves to the lateral loading $p_n(z)$ as shown in Fig. 5.

Consider the case of a shell subjected to a concentrated flattening force P_κ^* and a concentrated bimoment M_ω^* applied at $\bar{\xi}$ (Fig. 8). For all points $\xi < \bar{\xi}$ relation (4.8) remains valid. For points $\xi > \bar{\xi}$ due to the linearity of the transformation one has

$$\begin{aligned}\omega(\xi) = {} & \omega_0 F_{\omega\omega}(\xi) + \kappa_0 F_{\omega\kappa}(\xi) + m_0 F_{\omega m}(\xi) + q_0 F_{\omega q}(\xi) \\ & + M_\omega^* F_{\omega m}(\xi - \bar{\xi}) + P_\kappa^* F_{\omega q}(\xi - \bar{\xi})\end{aligned} \tag{4.11}$$

etc.

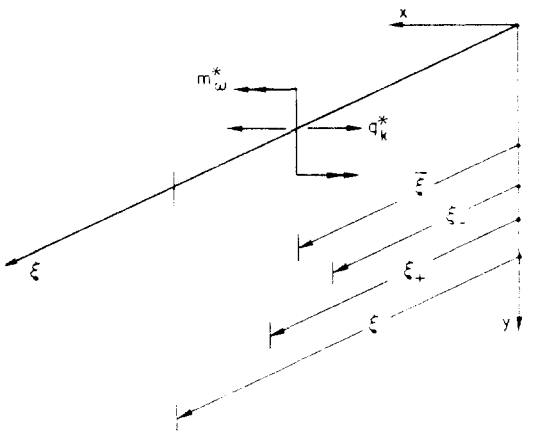

FIG. 8. Concentrated bimoment and flattening load applied at $\xi = \bar{\xi}$.

In matrix notation

$$\{s\}_\xi = [F(\xi)]\{s_0\} + \{s^0\}. \tag{4.12}$$

In a general case of a load distributed over some length (ξ_-, ξ_+) it follows that the components of the vector $\{s^0\}$ are

$$\begin{aligned}\omega^0 &= \int F_{\omega q}(\xi - \eta)\bar{P}_\kappa(\eta)\,d\eta + \int F_{\omega m}(\xi - \eta)m_\omega^*(\eta)\,d\eta \\ \kappa^0 &= \int F_{\kappa q}(\xi - \eta)\bar{P}_\kappa(\eta)\,d\eta + \int F_{\kappa m}(\xi - \eta)m_\omega^*(\eta)\,d\eta \\ m^0 &= \int F_{mq}(\xi - \eta)\bar{P}_\kappa(\eta)\,d\eta + \int F_{mm}(\xi - \eta)m_\omega^*(\eta)\,d\eta \\ q^0 &= \int F_{qq}(\xi - \eta)\bar{p}_\kappa(\eta)\,d\eta + \int F_{qm}(\xi - \eta)m_\omega^*(\eta)\,d\eta\end{aligned} \tag{4.13}$$

where F_{ij} are the corresponding components of the field transfer matrix [F] (4.9). The domain of integration is $[\xi_-, \xi_+]$. Formulas (4.13) are apparently also valid for concentrated loads when the integrals (4.13) are interpreted in Stieltjes sense or, even simpler, if the loads are presented by Dirac-delta function $\delta(\xi)$.

$$P_\kappa^*(\bar{\xi}) = \bar{p}_\kappa(\xi)\delta(\xi - \bar{\xi}).$$

For a flattening force $\bar{p}_\kappa = P^*$ uniformly distributed over the entire length $(0, L)$ of the shell, from (4.13) it follows that

$$\{s^0\} = p^* \begin{Bmatrix} \Delta(\alpha F_1^* - \beta F_3^*) \\ -(F_2^* + \gamma F_4^* - 1) \\ \dfrac{F_4^*}{2\alpha\beta} \\ \dfrac{\alpha F_1^* + \beta F_3^*}{2\alpha\beta} \end{Bmatrix} \tag{4.14}$$

where asterisk in F_i^* denotes the value of F_i for $\xi = 1$. With p^* denoted is the intensity of the nondimensionalized external distributed flattening load.

For a concentrated flattening force Q^* at $\xi = 0{\cdot}5$ it follows

$$\{s^0\} = P_\kappa^* \begin{Bmatrix} -\dfrac{1}{2\alpha\beta} F_4(0{\cdot}5) \\ -\dfrac{1}{2\alpha\beta}[a_3 F_1(0{\cdot}5) + b_3 F_3(0{\cdot}5)] \\ \dfrac{1}{2\alpha\beta}[\alpha F_1(0{\cdot}5) + \beta F_3(0{\cdot}5)] \\ F_2(0{\cdot}5) + \gamma F_4(0{\cdot}5) \end{Bmatrix}. \tag{4.15}$$

We note that the terms arrayed into vector $\{s^*\}$ in (4.12) are nothing but particular integrals. The proof is rather straightforward. Going along the negative ξ axis one may write

$$\{s_0\} = [\bar{F}]\{s_\xi\} \tag{4.16}$$

where the matrix $[\bar{F}]$ is obtained from $[F]$ given by (4.9) by replacing ξ through $-\xi$. This amounts to changing sign in front of odd functions F_1 and F_3. By comparison of (4.8) and (4.16) it follows that

$$[\bar{F}] = [F]^{-1} \tag{4.17}$$

Equations (3.8) and (3.23) are further rewritten as

$$\begin{aligned} \omega' + m &= 0 \\ \kappa' + 2r^2 q + s^4 \omega &= 0 \\ m' - q &= 0 \\ q' + \kappa &= \bar{p}_\kappa. \end{aligned} \tag{4.18}$$

Using now the method of variations of constants in conjunction with (4.17) it follows that $\{s^0\}$ are indeed particular integrals.

5. STRESSES IN THE SHELL

As a result of adopted assumptions the problem is decomposed into two parts. First part consists of the beam-like behavior of the shell (Bernoulli's hypothesis of planar cross section preserved), while the second part accounts for the distortion of the cross section. Therefore, total stresses in the shell are determined by superposition of stresses due to the flexure of the shell regarded as beam, and stresses due to the distortion of the cross section (departure from the Bernoulli's hypothesis).

For the purpose of comparison we will restrict ourselves to uniformly distributed load p_n (Fig. 5) extending over the entire length of the shell. The load components p_{s1} (beam type bending) and p_{s2} (flattening effect) are given by (3.3). Moreover, we will assume that the shell is simply supported $V_1 = M_y = 0$ at both ends $z = 0, L$.

(i) The normal stress σ_z due to the beam type bending is

$$\sigma_z^{(b)} = \frac{M_y}{I_y} y$$

where the bending moment (for uniformly distributed load $p_{s1} = 2p_n l$ in lb in.$^{-1}$) is

$$M_y = p_n l z(L - z).$$

Moment of inertia I_y is

$$I_y = \int_A y^2 \, dA = \frac{10}{3} l \, dh^2.$$

For $y = \pm h$ and $z = 0{\cdot}5L$ the maximum stress is

$$\sigma_z^{(b)} = \mp \frac{\sqrt{3}}{20} p_n \frac{L^2}{dl} \tag{5.1}$$

where superscript (b) refers to bending. Upper sign ($-$ for compression) is for the upper plate (1–6), while the lower sign ($+$ for tension) is related to the bottom plate (3–4).

The normal stress σ_z due to the "warping" of the cross section is according to (3.16)

$$\sigma_z^{(w)} = \frac{M_\omega(z)}{I_\omega} \Omega(s) \tag{5.2}$$

where $\Omega = \phi_3$ (Fig. 3) is the sectorial coordinate. Since for every $z = \text{const.}$ M_ω, I_ω is a constant, the distribution of $\sigma_z^{(w)}$ in the cross section is defined by Ω.

As a result of our analysis we will be able to compute nondimensional bimoments $\bar{m}_\omega$, flattening forces $\bar{q}$ and distortions $\bar{\kappa}$. Bar denotes that the corresponding quantity is computed for $q^* = 1$.

Once the nondimensional moment $\bar{m}_\omega(\alpha, \beta, \xi)$ is computed, according to (3.21a), (3.22) and (3.3) it follows that

$$M_\omega = \bar{m}_\omega p_n L^2 = \tfrac{3}{2} \bar{m}_\omega p_n L^2 l h. \tag{5.3}$$

Therefore for both upper and bottom plates

$$\sigma_z^{(w)} = \frac{9}{4}\bar{m}_\omega p_n \frac{L^2}{dh^3}\Omega = \frac{3}{4}\bar{m}_\omega p_n \frac{L^2}{dh}. \tag{5.4}$$

We note that for points $y = 0$, $x = \pm l$ (i.e. in the horizontal plane through the neutral line)

$$\sigma_z^{(b)} = 0 \quad \text{and} \quad \sigma_z^{(w)} = -\frac{3}{2}\bar{m}_\omega p_n \frac{L^2}{dh}. \tag{5.5}$$

(ii) The flattening force Q_κ is calculated from (3.21b), (3.22) and (3.3) to be

$$Q_\kappa = \bar{q} p_\kappa L = \tfrac{3}{2}\bar{q} p_n l h L. \tag{5.6}$$

For $K = \frac{1}{2}Al$ and for $\Psi = \pm(\sqrt{3}/2)l$ (Fig. 4) it follows from (3.18) that the shear stress due to the distortion of the cross section is

$$\tau^{(d)} = \pm\frac{\sqrt{3}}{4}\bar{q} p_n \frac{L}{d} \tag{5.7}$$

where the distribution in the cross section is defined by $\Psi = \psi_2$ (Fig. 4).

The shear stresses due to the beam type behavior of the shell, to be superimposed on (5.7), are

$$\tau^{(b)} = \frac{Q_z}{s} b \tag{5.8}$$

where Q_z is the transverse force, s cross-sectional modulus and b thickness of the relevant part of the cross section measured parallel to x-coordinate.

(iii) In addition to these two stresses, the circumferential normal stress σ_s due to the flattening of the cross sectional frame ought to be determined. The bending moments at nodal points of the cross section regarded as a hexagonal frame (Fig. 6) are according to (3.2)

$$M_s(z) = \frac{12}{5}\frac{EI_y}{l}\frac{h}{l}\kappa_1(z). \tag{5.9}$$

Once the flattening of the cross section $\bar{\kappa}(z)$ (again for $q^* = 1$) is solved for, it follows that

$$M_s = \frac{3}{16}\bar{\kappa} p_n l^2.$$

The normal stresses in the upper and lower fibres are

$$\sigma_s^{(f)} = \pm\frac{M}{I_y}\frac{d}{2} = \pm\frac{9}{8}\bar{\kappa} p_n \frac{l^2}{d}. \tag{5.10}$$

Relation (5.10) would give the total hoop stress for the load linearly distributed along the nodal lines. For the load presented in Fig. 6(a), additional hoop stresses are determined from the hexagonal frame subjected to balanced load from the Fig. 6(b). The maximum bending moment in the frame occurs at nodes 1 and 6

$$M_s = \frac{5}{72} p_n l^2, \sigma_s = \frac{5}{12} p_n \frac{l^2}{d}. \tag{5.11}$$

Hence, the total hoop stress is

$$\sigma_s^{(f+b)} = \mp\left(\frac{9}{8}\bar{\kappa}+\frac{5}{12}\right)p_n\left(\frac{l}{d}\right)^2 \tag{5.12}$$

where the upper sign belongs to the upper fibre.

6. EXAMPLES

As an illustration of the method, the results of the analysis of shells with various geometries and boundary conditions will be presented. Shells are loaded by a uniformly distributed external load p_n (as in Fig. 5) along the entire length $0 \leq z \leq L$. The analysis is carried out for three sets of boundary conditions, namely, the terminal cross sections at $z = 0$ and L are:

(a) Stiffened by a thin diaphragm being rigid in its own plane, but offering no resistance to deformations perpendicular to the cross section, i.e. at $z = 0, L$

$$\kappa = M_{zz} = 0. \tag{6.1}$$

(b) Stiffened by a thick diaphragm which cannot deform at all, i.e. at $z = 0, L$

$$\kappa = \omega = 0. \tag{6.2}$$

(c) Completely free, i.e. at $z = 0, L$

$$M_{zz} = Q_\kappa = 0. \tag{6.3}$$

6.1 *Thin diaphragm*

Boundary conditions are given by (6.1). Two initial conditions are known $\kappa_0 = m_0 = 0$. The remaining two ω_0, q_0 are determined from $\kappa(1) = m(1) = 0$, i.e. from (4.9) and (4.14) one has in matrix notation

$$\begin{bmatrix} -(\alpha^2+\beta^2)^2(\alpha F_1^* + \beta F_3^*) & -(a_3 F_1^* + b_3 F_3^*) \\ (\alpha^2+\beta^2)(\alpha F_1^* - \beta F_3^*) & (\alpha F_1^* + \beta F_3^*) \end{bmatrix} \begin{Bmatrix} \omega_0 \\ q_0 \end{Bmatrix} = p^* \begin{Bmatrix} 2\alpha\beta(F_2^* + \gamma F_4^* - 1) \\ -F_4^* \end{Bmatrix} \tag{6.4}$$

where $(2\alpha\beta)^{-1}$ is factored out. From (6.4) it follows

$$\begin{aligned} \omega_0 &= -p^* \frac{(\coth\alpha - c_2)(\beta - c_1)}{2\alpha\beta(\alpha^2+\beta^2)(1+c_1^2)} \\ q_0 &= -p^* \frac{(\coth\alpha - c_2)(\beta + \alpha c_1)}{2\alpha\beta(1+c_1^2)} \end{aligned} \tag{6.5}$$

where

$$c_1 = \frac{\sin\beta}{\sinh\alpha} \qquad c_2 = \frac{\cos\beta}{\sinh\alpha}. \tag{6.6}$$

Once ω_0 and q_0 are determined we calculate the generalized forces from (4.9) and (4.14) to be

$$\frac{1}{p^*}m_\omega = \bar{m}_\omega = \frac{\alpha^2+\beta^2}{2\alpha\beta}(\alpha F_1 - \beta F_3)\omega_0 + \frac{1}{2\alpha\beta}(\alpha F_1 + \beta F_3)q_0 + \frac{F_4}{2\alpha\beta} \tag{6.7}$$

$$\frac{1}{p^*}q = \bar{q} = \frac{(\alpha^2+\beta^2)^2}{2\alpha\beta}F_4\omega_0 + (F_2+\gamma F_4)q_0 + \frac{\alpha F_1 + \beta F_3}{2\alpha\beta} \tag{6.8}$$

while the flattening deformation is

$$\frac{1}{p^*}\kappa = \bar{\kappa} = -\frac{(\alpha^2+\beta^2)^2}{2\alpha\beta}(\alpha F_1 + \beta F_3)\omega_0 - \frac{1}{2\alpha\beta}(a_3F_1 + b_3F_3)q_0 - (F_2+\gamma F_4 - 1). \tag{6.9}$$

It is obvious that the relation (6.7), for example, could be still simplified. From (6.5) and (6.7) it follows that

$$\bar{m}_\omega(\xi) = -\frac{(\coth\alpha - c_2)}{2\alpha\beta}(\alpha F_1 - \beta F_3)(F_1 + c_1F_3) + \frac{F_4}{2\alpha\beta} \tag{6.10}$$

etc.

The diagrams $\bar{m}_\omega(\xi)$, $\bar{q}(\xi)$ and $\bar{\kappa}(\xi)$ are plotted in Figs. 9–11. We note from the diagrams in Fig. 9 that the bimoments in the midspan become negligible with increase of the relative length ratio L/l. In fact for large $\rho = L/l$ it follows that $s^2 \gg r^2$. Therefore, $\alpha \sim \beta$, $c_1 \sim 0$, $c_2 \sim 0$ and $\coth\alpha \sim 1$. From (6.5) it follows that

$$\begin{aligned} \omega_0 &= -\frac{p^*}{2\alpha(\alpha^2+\beta^2)} = -\frac{p^*}{4\alpha^3} \\ q_0 &= -\frac{p^*}{2\alpha} \end{aligned} \tag{6.11}$$

Writing now

$$F_1 = \tfrac{1}{2}\sin\alpha\xi(e^{\alpha\xi} + e^{-\alpha\xi}) \qquad \text{etc.}$$

it follows that the distribution of bimoments is given by

$$\bar{m}_\omega = -\left(\frac{1}{2\alpha^2}\sin\alpha\xi\right)e^{-\alpha\xi} \tag{6.12}$$

In other words the bimoments are rapidly decaying going away from the diaphragm which is typical of the so-called edge effect. We, of course, realize that the omission of M_z as an internal force in our analytical model, does not allow for an accurate assessment of stresses near the ends.

6.2 *Thick diaphragms*

As a next case we consider boundary conditions (6.2). Two unknown initial parameters m_0 and g_0, are calculated from

$$\begin{bmatrix} \dfrac{a_3F_1^* - b_3F_3^*}{\alpha^2+\beta^2} & -F_4^* \\ (\alpha^2+\beta^2)^2F_4^* & -(a_3F_1^* + b_3F_3^*) \end{bmatrix} \begin{Bmatrix} m_0 \\ q_0 \end{Bmatrix} = \begin{Bmatrix} \dfrac{1}{\alpha^2+\beta^2}(\alpha F_1^* - \beta F_3^*) \\ 2\alpha\beta(F_2^* + \gamma F_4^* - 1) \end{Bmatrix} \tag{6.13}$$

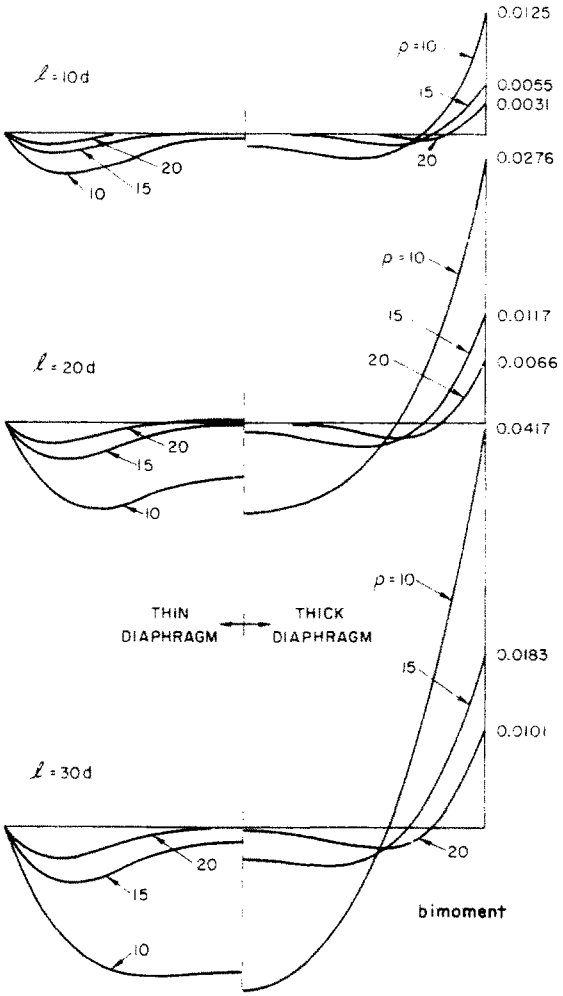

FIG. 9. Nondimensional bimoments for $l/d = 10, 20, 30$ and $L/l = 10, 15, 20$. Left thin diaphragms case, right thick diaphragms case.

such that

$$\frac{1}{p^*} m_0 = \frac{\beta - \alpha c_1}{b_3 - a_3 c_1}$$

and (6.14)

$$\frac{1}{p^*} q_0 = \frac{2\alpha\beta(c_2 - \coth \alpha)}{b_3 - a_3 c_1}$$

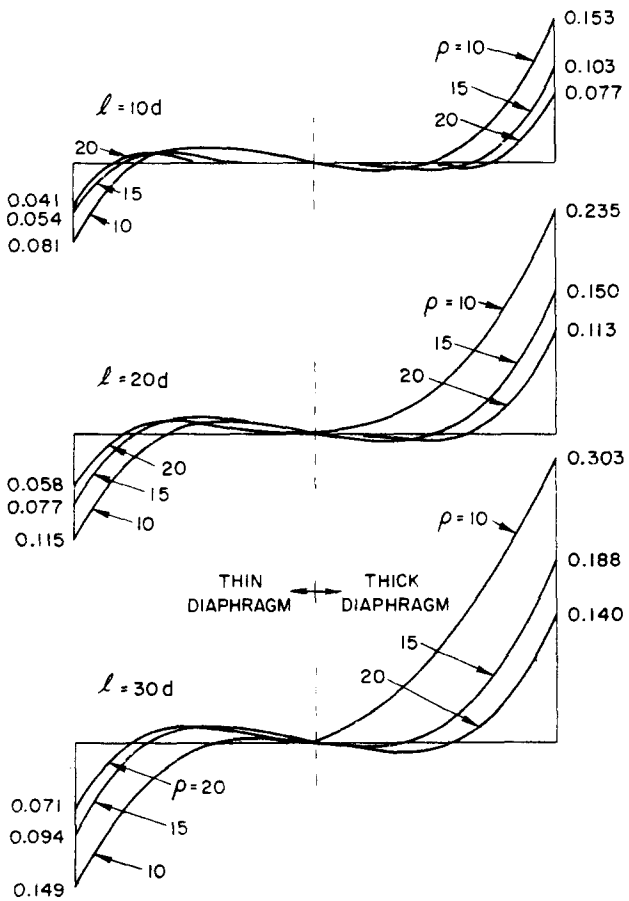

FIG. 10. Nondimensional flattening force for $l/d = 10, 20, 30$ and $L/l = 10, 15, 20$. Left thin diaphragms case, right thick diaphragms case.

such that

$$\frac{1}{p^*}m_\omega = \bar{m} = (F_2 - \gamma F_4)m_0 + \frac{1}{2\alpha\beta}(\alpha F_1 + \beta F_3)q_0 + \frac{F_4}{2\alpha\beta} \tag{6.15}$$

$$\frac{1}{p^*}q_\kappa = \bar{q} = -\frac{\alpha^2+\beta^2}{2\alpha\beta}(\alpha F_1 - \beta F_3)m_0 + (F_2 + \gamma F_4)q_0 + \frac{1}{2\alpha\beta}(\alpha F_1 + \beta F_3) \tag{6.16}$$

$$\frac{1}{p^*}\kappa = \bar{\kappa} = \frac{(\alpha^2+\beta^2)^2}{2\alpha\beta}F_4 m_0 - \frac{1}{2\alpha\beta}(a_3 F_1 + b_3 F_3)q_0 - (F_2 + \gamma F_4 - 1). \tag{6.17}$$

For long and thin shells, using same arguments as in the Section 6.1, we derive

$$m_0 = \frac{1}{2\alpha^2}p^* \quad \text{and} \quad q_0 = -\frac{1}{\alpha}p^*$$

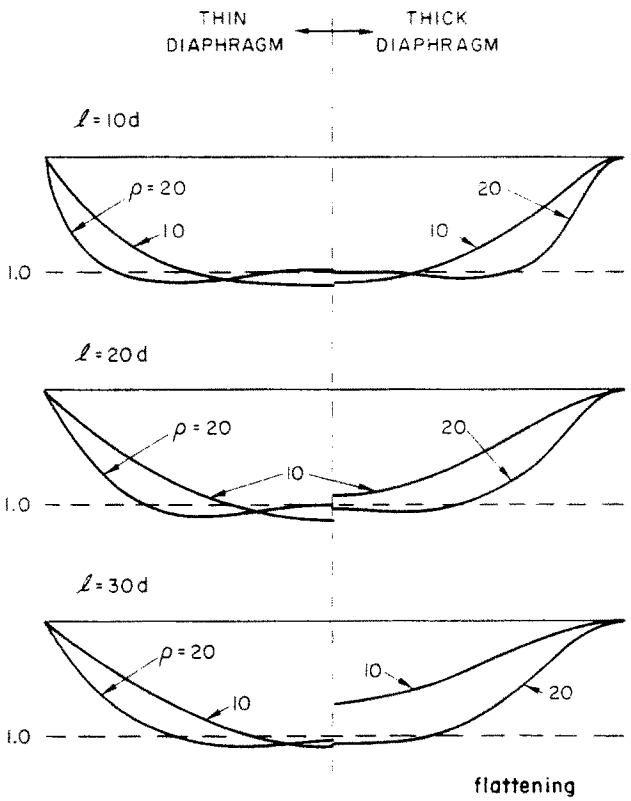

FIG. 11. Nondimensional flattening for $l/d = 10, 20, 30$ and $L/l = 10, 20$. Left thin diaphragms case, right thick diaphragms case.

and the distribution of bimoments is therefore

$$\bar{m} = \frac{1}{2\alpha^2} e^{-\alpha\xi}(\cos\alpha - \sin\alpha). \tag{6.18}$$

6.3 *Free ends*

From boundary conditions (6.3) $m_0 = g_0 = 0$. Two remaining initial parameters are computed from $m(1) = g(1) = 0$

$$\begin{bmatrix} (\alpha^2+\beta^2)(\alpha F_1 - \beta F_3) & -F_4 \\ (\alpha^2+\beta^2)^2 F_4 & -(\alpha F_1 - \beta F_3) \end{bmatrix} \begin{Bmatrix} \omega_0 \\ \kappa_0 \end{Bmatrix} = -p^* \begin{Bmatrix} F_4 \\ \alpha F_1 + \beta F_3 \end{Bmatrix} \tag{6.19}$$

The solution of (6.15) is by inspection

$$\omega_0 = 0 \qquad \kappa_0 = p^* \tag{6.20}$$

such that

$$\bar{\omega} = \bar{m} = \bar{q} = 0 \tag{6.21}$$

and

$$\bar{\kappa} = p^*. \tag{6.22}$$

Diagrams of the bimoment, flattening force and flattening itself are presented in Figs. 9–11.

As expected, an unstiffened shell subjected to uniformly distributed flattening load undergoes only a uniform flattening of the cross section, while the "warping" is absent. As a consequence, stresses $\sigma_z^{(w)} \equiv \tau^{(d)} \equiv 0$, while $\sigma_s^{(f)}$ may be computed directly as for the hexagonal frame (Fig. 6).

7. CONCLUSIONS

Some important conclusions follow from computed results. In almost all cases the influence of diaphragms on prevention of flattening has local character. In other words, the flattening of the cross section, and therefore, hoop normal stresses σ_s are in the midspan equal as for the unstiffened case. On the other hand, by constraining warping, diaphragms induce bimoments, and consequently, add to the normal stresses σ_z. Hence, in particular case diaphragms should be either very close or avoided at all (if σ_s are not considered significant). In order to get a feeling for the order of magnitude of stresses we present a few results. With regard to classical bending the shell is simply supported at $\xi = 0, 1$.

For $l = 10d$ and $L = 10l$, at the midspan $\bar{m} = 0{\cdot}00030$ and $\bar{k} = 1{\cdot}090$ for the case of the thin diaphragm. Hence, in the bottom plate

$$\max \sigma_z^{(w+b)} = (0{\cdot}26 + 103{\cdot}92)p_n$$

while

$$\max \sigma_s^{(f+b)} = (122{\cdot}7 + 41{\cdot}7)p_n$$

i.e. the normal hoop stresses due to the distortion of the cross section exceed the longitudinal normal stresses (with warping contributing a quarter of a per cent).

However, for the same case but $l = 30d$, $\bar{m} = 0{\cdot}0149$ such that

$$\max \sigma_z^{(w+b)} = (38{\cdot}83 + 103{\cdot}92)p_n$$

Maximum normal stress due to the "warping" occurs for thick diaphragms at $\xi = 0, 1$. For $L = 10l$ and $l = 30d$, $\bar{m}(\xi = 0) = -0{\cdot}0417$. Hence

$$\sigma_z^{(w)} = -108{\cdot}26p_n$$

Now if the shell is fully clamped with respect to bending, at the same place we compute

$$\sigma_z^{(b)} = -103{\cdot}92p_n$$

again in the bottom plate. In this case the contribution of bending and warping are just about equal.

One should keep in mind that this discussion is restricted to the uniformly distributed load. In case of a concentrated force even for the shell without diaphragms warping will occur and the conclusions may be quite different.

One can summarize the computed results in the following way. If the shell is long enough the longitudinal normal stresses σ_z due to the beam type of bending are predominant and little is to be gained by suppressing cross-sectional distortions, especially if σ_s is within allowable limits.

Due to the simplicity of the procedure and availability of closed form solutions a thorough parametric analysis appears to be quite appropriate for each given case.

8. SUMMARY

Presented is a static stress analysis of a long prismatic shell with a hexagonal cross section. The method employed is known as semimembrane, implications of which are discussed in Section 1. Such a formulation enables a closed form solution to the problem. The analysis is decomposed into two parts:

(a) analysis of the shell regarded as a beam (see Ref. [7]);
(b) determination of additional stresses and strains due to the departure ("warping" and flattening) from the beam behavior of the shell.

The proposed method of analysis stands, therefore, in between the exact (shell theory) solution and the approximate "beam" type of solution. If necessary, we can improve on the accuracy by adding new deformation modes. In the close proximity of diaphragms the results for stresses are incomplete due to the absence of bending moment M_z. However, in most cases maximum stresses are located in the middle of the shell where the proposed method is a close approximation of exact theory.

Solution to the problem, presented in Sections 3–6, is formulated in form of the initial parameters (or transfer matrices) method. This type of formulation enables the analysis of a much wider scope of problems than it was possible to outline in a single paper.

Acknowledgement—The author wishes to acknowledge some useful suggestions offered by G. S. Rosenberg, A.N.L.

REFERENCES

[1] Phase I Report on Folded Plate Construction, Report of the Task Committee on Folded Plate Construction. *J. struct. Div. Am. Soc. civ. Engrs* **89**, 365 (1963).
[2] V. Z. VLASOV, General Theory of Shells and Its Applications in Engineering, Part V. NASA Translation N64–19883 Washington (1964).
[3] I. F. OBRAZCOV, *Variational Methods of Analysis of Thinwalled Airplane Structures*, (in Russian). Mashinostroenie (1966).
[4] C. F. KOLLBRUNNER and N. HAJDIN, *Woelbkrafttorsion duenwandiger Staebe mit geschlossenem Profil*. Schweizer Stahlbau-Vereinigung, Mitt. der Tech. Kommision. Heft 32, Zurich (1966).
[5] D. KRAJCINOVIC, A consistent discrete element technique for thinwalled assemblages. *Int. J. Solids Struct* **5**, 639–662 (1969).
[6] E. C. PESTEL and F. A. LECKIE, *Matrix Methods in Elastomechanics*. McGraw-Hill (1963).
[7] E. H. BAKER, A. P. CAPPELLI, L. KOVALEVSKY, F. L. RISH and R. M VERETTE, Shell Analysis Manual. NASA publication N68-24802, Washington D.C. (1968).

(*Received* 20 *February* 1970; *revised* 16 *July* 1970)

Абстракт—Исследуется, обыкновенным методом, анализ напряжений длинных призматических оболочек с гексагональными поперечными сеуениями, подверженных действию статической нагрузки. Получается решение, в замкнутом виде, применяя метод полумембраны вместе с вариационным принципом. Поэтому, можно легко выполнить исследование параметров разных геометрий и граничных условий, имея в наличии их влияние на напряженное состояние. Между прочим показано, что усиление оболочки поперечными диафрагмами не всегда целесообразно.